Photochemistry and Photobiology, 2005, 81: 1107–1115

Invited Review

Intercalation of Organic Dye Molecules into Double-stranded DNA. Part 2: The Annelated Quinolizinium Ion as a Structural Motif in DNA Intercalators†

Heiko Ihmels*[1], Katja Faulhaber[2], Daniela Vedaldi[3], Francesco Dall'Acqua[3] and Giampietro Viola[3]

[1]Institute of Organic Chemistry, University of Siegen, Siegen, Germany
[2]Institute of Organic Chemistry, University of Würzburg, Würzburg, Germany
[3]Department of Pharmaceutical Sciences, University of Padova, Padova, Italy

Received 25 January 2005; accepted 25 May 2005; published online 4 June 2005 DOI: 10.1562/2005-01-25-IR-427

ABSTRACT

DNA intercalators represent an important class of compounds with a high potential as DNA-targeting drugs. In this review it is demonstrated that annelated quinolizinium derivatives such as coralyne and derivatives thereof intercalate into DNA and that this structural motif allows several variations of the substitution pattern without loss of intercalating properties. The commonly applied methods for the evaluation of the DNA association, mainly spectroscopic studies, are pointed out. In addition, studies on the biological activities of annelated quinolizinium derivatives, such as topoisomerase poisoning or cell toxicity, are highlighted.

INTRODUCTION

Polycyclic aromatic molecules are known to intercalate into double-stranded DNA (1,2). Apart from the theoretical treatment of such host–guest interactions, the consequences of DNA intercalation by exogeneous molecules have attracted considerable interest in medicinal chemistry, because such a complex formation leads to a significant modification of the DNA structure and may result in a hindered or suppressed function of the nucleic acid in physiological processes (3–10). Because such an influence on the biological system is a main requirement for DNA-targeting drugs, the intercalation of small molecules into DNA may be applied in therapeutic approaches in which the suppression of DNA replication and gene transcription is used to destroy tumor cells or infected tissue. As a result, many studies have been performed to gain more insight in different aspects of the association process of large and small molecules with DNA in order to obtain highly selective and efficient intercalators (11).

Cationic organic dyes are usually regarded as classical intercalators. Representative examples are acridine derivatives such as proflavine (1) or acridine orange (12), azine dyes such as methylene blue (13), phenanthridinium salts such as ethidium bromide (14) or cyanine dyes such as thiazole orange (aggregates of which may also bind to the minor groove) (15–17). The association of these compounds with DNA usually influences their absorption and emission properties, so that their interaction with DNA may be evaluated qualitatively and quantitatively by spectrophotometric and spectrofluorometric titrations (18). These simple and straightforward spectroscopic methods are especially advantageous because organic dyes absorb and emit at wavelengths that do not interfere with the absorption of the DNA bases ($\lambda_{max} \approx 260$ nm). Thus, spectrophotometric and spectrofluorometric titrations usually indicate the association of a dye with DNA. Moreover, the resulting binding isotherms can be used to estimate the binding constants and the binding site size, *i.e.* the number of occupied binding sites. Moreover, the absorption of circularly or linearly polarized light can be used in circular dichroism (CD) and linear dichroism (LD) spectroscopy to gain further knowledge of the orientation of the dye molecule relative to the DNA and to deduce the binding mode (19). Steady-state fluorescence polarization measurements as well as fluorescence energy transfer from the DNA bases to the bound dye have been used as additional reliable criteria to elucidate the binding mode (20). In addition to the spectroscopic methods, hydrodynamic and thermodynamic criteria such as the viscosity, the sedimentation coefficient, or the DNA melting temperature may be used to evaluate the binding mode (20).

It is commonly established that a positive charge enhances the propensity of a molecule to bind to DNA due to attractive ionic interactions between the cation and the phosphate backbone (21). In most cationic dyes, this positive charge is established by an exocyclic ammonium functionality or by an endocyclic pyridinium moiety. These functionalities are usually quaternized by alkylation or protonation. In the latter case, however, this leads to a significant influence of the pH on the DNA-binding properties. In contrast, cationic dyes with an endocyclic quaternary *bridgehead* nitrogen atom are rather rare and few systematic studies exist for this class

* To whom correspondence should be addressed: Institute of Organic Chemistry, University of Siegen, Adolf-Reichwein-Str. 2, D-57068 Siegen, Germany. Fax: +49 (0) 271 740 2226; e-mail: ihmels@chemie.uni-siegen.de

† Part 1: Ihmels, H. and D. Otto. (2005) *Top. Curr. Chem.* **258**, 161–204.

Abbreviations: CD, circular dichroism; ct DNA, calf thymus DNA; DSC, differential scanning calorimetry; ICD, induced circular dichroism; LD, linear dichroism; st DNA, salmon testes DNA

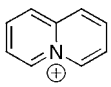

Quinolizinium Ion

Scheme 1.

of compounds. In this article we will summarize the studies of the DNA-binding properties of quinolizinium (Scheme 1) derivatives (22) as representative examples for dyes with a quaternary bridgehead nitrogen atom, and we will demonstrate that annelated quinolizinium derivatives may serve as a useful platform for the design of intercalating dyes.

CORALYNE

The main interest in DNA intercalators with a quinolizinium core stems from early studies of berberine derivatives such as coralyne (**1a**) and related alkaloids, which exhibit antileukemic activity (23). Although its antitumor activity is not very high, coralyne represents a promising lead structure along these lines because of its very low toxicity (24,25). Early work from Zee-Cheng and Cheng has already established the association of coralyne with DNA (26), which led to the assumption that the DNA interaction may be correlated with the biological activity.

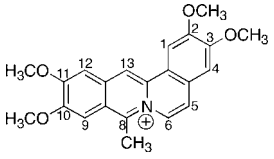

1a

A more detailed analysis by Wilson *et al.* showed that coralyne intercalates into DNA at low dye–DNA ratios (27,28). With an increasing dye–DNA ratio, however, coralyne molecules bind also by π-stacking along the DNA backbone. In a subsequent study, the binding selectivity of coralyne was studied by spectrophotometric and spectrofluorometric titrations, viscosimetric studies and CD spectroscopy with DNA duplexes with different GC-to-AT ratios (29). These experiments revealed that coralyne binds with a small but significant preference to GC-rich DNA regions.

In addition, coralyne was shown to bind to parallel triplex DNA; however, attempts to intercalate coralyne in antiparallel triplex DNA failed (30). Although it was concluded from early experiments (using thermal denaturation analysis and spectrophotometric titration) with TA•T- and CG•C^+-containing DNA triplexes that coralyne does not exhibit a significant sequence selectivity during triplex association (31), a later study (with DNase footprinting, thermal denaturation analysis, spectrometric titrations and CD and NMR spectroscopy) showed a preferential intercalation of coralyne into TA•T triplexes (32). According to the latter study, coralyne is fully intercalated into TA•T triplex DNA whereas in CG•C^+ triplexes the coralyne molecule is only partially intercalated due to the electrostatic repulsion between the cationic dye and the protonated cytosine. Most notably, the high propensity of coralyne to stabilize triplex DNA is nicely demonstrated by the observation that duplex poly(dT)-poly(dA) is transformed to a mixture of poly(dT)-poly(dA)-poly(dT) triplex DNA and single-stranded poly(dA) in the presence of coralyne at slightly elevated temperatures ($T > 35°C$). This disproportionation reaction of double-stranded DNA has been rationalized in terms of the formation of a highly stable intercalation complex between coralyne and triplex DNA (33,34). Recently, it was demonstrated that coralyne may act as a template for the formation of an antiparallel DNA duplex from homo-adenine sequences (35).

Although a wealth of data is presently available regarding the interactions of coralyne with DNA, the interpretation of these data needs to be performed with care. Unfortunately, coralyne exhibits a high tendency for aggregation in water, even at low concentrations. Therefore, aggregates of coralyne molecules are used in most experiments rather than separate independent molecules, which may have a significant influence especially on the optical properties of the system. Maiti *et al.* addressed this problem and showed that aqueous solutions, which contain 30% (v/v) ethanol, suppress the aggregation of coralyne and may allow spectrometric titrations with nonaggregated coralyne monomers (29). It was proposed that these concentrations of ethanol do not disturb the original DNA structure under these conditions (36).

Presumably, the most important biological feature of coralyne, which is directly connected to the DNA-intercalating properties, is its ability to act as a human topoisomerase I poison. Topoisomerases are essential DNA-targeting enzymes that initially induce a DNA-strand cleavage, followed by a DNA-strand reorganization and reconnection (37,38). The result of this process is the relaxation of the DNA structure, which is required *e.g.* during transcription or replication processes. In the presence of so-called topoisomerase poisons, a ternary complex between DNA, an intercalator and topoisomerase is formed. This ternary complex is more stable than the DNA–topoisomerase associate, which may lead to an enhanced lifetime of the initially cleaved DNA. As a consequence, the religation of the strands cannot take place, *i.e.* the strand breaks remain permanent, so that the topoisomerase acts as an endogenous poison under these circumstances. Therefore, compounds that form such stable ternary complexes with DNA and topoisomerase exhibit a high potential as DNA-targeting anticancer drugs. By a different mechanism, topoisomerase inhibitors suppress the association of topoisomerase with DNA, and thus the topoisomerase activity, by the occupation of the corresponding binding site.

Hecht *et al.* demonstrated that a number of protoberberine-type alkaloids, including the antitumor agent coralyne (**1a**), also inhibit topoisomerase I function (39). Thus, coralyne and the partially saturated derivative 5,6-dihydrocoralyne (**1b**) both stabilize the complex between topoisomerase I and DNA. At high concentra-

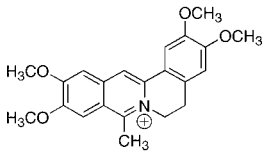

1b

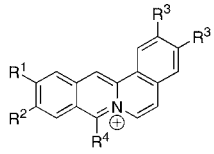

1c–**1j**

1c: $R^1 = R^2 = R^3 = OCH_3$; $R^4 = H$
1d: $R^1 = R^2 = R^3 = OCH_3$; $R^4 = CH_2CH_2CH_3$
1e: $R^1 = R^2 = R^3 = OCH_3$; $R^4 = CH_2CH_2OH$
1f: $R^1 = R^2 = R^3 = OCH_3$; $R^4 = CH_2CH_2COOH$
1g: $R^1 = R^4 = H$; $R^2 = R^3 = OCH_3$
1h: $R^1 = OH$; $R^2 = R^3 = OCH_3$; $R^4 = H$
1i: $R^1 = R^3 = OCH_3$; $R^2 = R^4 = CH_3$
1j: $R^1 = R^2 = R^3 = -OCH_2O-$; $R^4 = CH_3$

tion, 5,6-dihydrocoralyne is almost as effective at stabilizing the binary complex as the known topoisomerase-poison camptothecin (40), an alkaloid that is frequently used as a standard reference to evaluate the relative topoismerase-poisoning activity. In contrast, coralyne was more effective than 5,6-dihydrocoralyne at lower concentrations. In addition, several coralyne derivatives, *e.g.* **1c–j**, were tested with respect to their ability to induce single-strand cleavage by the formation of ternary complexes with plasmid DNA and topoisomerase I. Although the derivatives **1c–j** also induce cleavage in pSP64 plasmid DNA, as monitored by the formation of the relaxed circular form II, these derivatives are not as efficient as coralyne or 5,6-dihydrocoralyne. Most notably, the coralyne-topoisomerase I–induced DNA cleavage is site-selective. Thus, preferential single-strand scission was observed between particular nucleotides in definite sequences. The site selectivity resembles that of camptothecin, however, additional cleavage was observed between the T and A residues in the sequence 5′-TCTCGTAA-3′. In a following study, Pilch *et al.* confirmed that 8-desmethylcoralyne (**1c**), 5,6-dihydro-8-desmethylcoralyne (**1k**), and palmatine (**1l**) may also act as topoisomerase I poisons, whereas no topoisomerase II poisoning properties were observed (41).

A comparison of the topoisomerase I-poison efficiency showed that **1k** is the most potent compound. The activity of **1c** is significantly

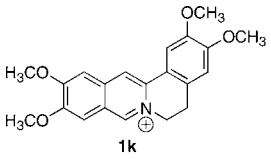

1k

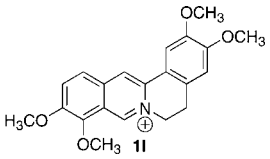

1l

lower, whereas palmatine (**1l**) exhibits only very weak activity as a topoisomerase I poison. Studies on the binding geometry of the DNA–protoberberine complex by absorption and LD spectroscopy, DSC analysis and microcalorimetry revealed a ''mixed-mode'' DNA binding model for these derivatives, in which one part of the aromatic system intercalates into the DNA double helix, while the nonintercalated moiety protrudes into the minor groove of the host duplex. Thus, the latter is available for associative interactions with other external molecules, such as the topoisomerase, that bind in the grooves. These experimental results were confirmed by theoretical modeling studies. Notably, the proposal of intercalative binding of palmatine was contradicted by hydrodynamic studies, which have shown that the viscosity of aqueous DNA solutions does not significantly change upon palmatine addition (42). Moreover, the fluorescence of DNA-bound palmatine is efficiently quenched by external additives such as potassium ferrocyanide. Because both observations indicate minor-groove binding, a corresponding binding mode was proposed for palmatine.

To gain more insight into the correlation between the structure and activity of coralyne-based topoisomerase I poisons, the influence of the substitution pattern of coralyne derivatives on their activity as topoisomerase poisons was studied with derivatives **1m–q** and **1a** (43). It was observed that those derivatives with a methylenedioxy functionality, *i.e.* **1n** and **1q**, exhibit the same activity as the known topoisomerase I poison coralyne (**1a**) (determined as the relative effective concentration required to induce the same plasmid–DNA cleavage as camptothecin), whereas **1m** and **1p** did not exhibit significant activity as topoisomerase I poisons. It was deduced that the methylenedioxy substitution may be a common factor associated with this property. Moreover, the significant influence of the saturation at positions 5 and 6 and the substituent in position 8 was demonstrated with derivative **1r**, which is, compared to the other derivatives studied, the most efficient topoisomerase I poison with a similar activity as camptothecin. Most notably, the derivatives **1n**, **1o** and **1q** also induce topoisomerase II-mediated DNA cleavage, with **1o** being the only derivative with 2,3-dimethoxy substitution that exhibits no significant activity as topoisomerase I poison. In addition, the cell toxicity of **1m–q** was investigated. Interestingly, no correlation was observed between cytotoxicity of the coralyne derivatives and their activity as topoisomerase poisons. It was assumed that the cationic charge as well as the structural rigidity of these derivatives may limit their cellular absorption and thus reduce their cytotoxic activity.

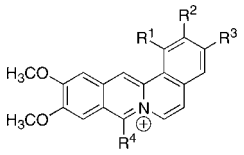

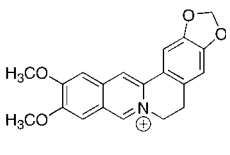

1r

1m: R^1 = H; R^2 = R^3 = OCH_3; R^4 = CH_3
1n : R^1 = H; R^2 = R^3 = $-OCH_2O-$; R^4 = CH_3
1o : R^1 = R^2 = OCH_3; R^3 = R^4 = H
1p : R^1 = R^4 = H; R^2 = R^3 = OCH_3
1q : R^1 = R^4 = H; R^2 = R^3 = $-OCH_2O-$

ANNELATED QUINOLIZINIUM DERIVATIVES

Although it has been shown by the results with coralyne that annelated quinolizinium derivatives may be a promising lead structure for DNA-intercalating drugs, the first example of a quinolizinium derivative without coralyne-like structure was reported in 1984 (44). As was coralyne, sempervirine (**2**), a naturally occurring alkaloid, was investigated with respect to its DNA-binding properties. Spectrophotometric titrations revealed that this alkaloid binds to DNA; however, these experiments showed also that sempervirine tends to form π-stacked aggregates on the DNA backbone, whose absorption distorts the titration spectra. Equilibrium-dialysis experiments showed that free sempervirine molecules are present in solution at polynucleotide-to-dye ratios of up to 4.

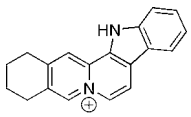

2

Electric dichroism measurements and viscosimetric studies gave evidence for an intercalative binding model, which takes place along with the backbone association. Although the extent of DNA unwinding upon sempervirine addition is rather small as compared to ''classical'' intercalators, the authors point out that the backbone aggregation also needs to be considered. Thus, a correction of the actual free-dye concentration led to a relative unwinding that is fully consistent with the formation of an intercalation complex.

The first study of DNA-binding properties of a series of non-natural quinolizinium derivatives with varying annelation pattern was reported in 1988 (45). Thus, the interaction of quinolizinium salts **3–8** with DNA was studied by absorption and emission spectroscopy. The absorption bands of all derivatives exhibit

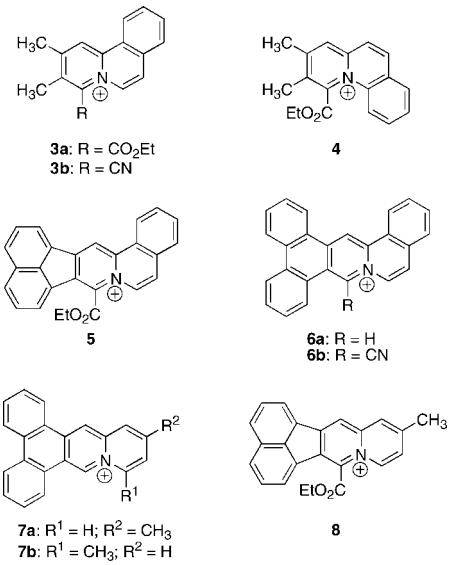

a significant redshift upon DNA addition along with a hypsochromic effect, *e.g.* the long-wavelength absorption of **5** changes from 415 nm to 425 nm. The fluorescence bands of some derivatives are also quenched in the presence of DNA but the quenching efficiency varies depending on the substitution pattern. The fluorescence of **5**, **7a** and **8** is significantly quenched in the presence of DNA, whereas the emission intensity of **3a**, **3b** and **4** remained essentially unchanged upon DNA addition. Unfortunately, quenching rates were not given and the different emission quenching in the presence of DNA was not discussed in detail. Additional evidence for strong DNA association of ions **3a**, **4** and **5** was obtained from viscosimetric studies, because the viscosity of DNA solutions increases upon addition of these quinolizinium derivatives. The binding mode of the quinolizinium derivatives **3–8** with DNA was not determined in this study.

Recently, the interactions of DNA with the benzo-, naphtho-, and indolo-annelated quinolizinium derivatives **9–12** were investigated in detail (46–53). As already shown for **5**, the absorption bands of quinolizinium derivatives **9–12** are significantly redshifted upon addition of calf thymus DNA (ct DNA) or salmon testes DNA (st DNA) (Table 1). The same effect was observed upon addition of synthetic double-stranded polynucleotides (poly[dC–dG]–poly[dC–dG]) and (poly[dA–dT]–poly[dA–dT]). Figure 1 shows exemplarily the photometric titrations of DNA to quinolizinium derivatives **9b** and **9c**.

Almost all quinolizinium derivatives **9–12** are fluorescent, and except for **9b**, the fluorescence intensity of the quinolizinium ions is efficiently quenched upon complex formation with DNA due to a photoinduced electron-transfer reaction between the excited quinolizinium derivative and the nucleic bases (54). Figure 2A shows exemplarily the spectrofluorometric titration of **12** (47). In contrast, the amino-substituted benzoquinolizinium **9b** is only weakly fluorescent due to a radiationless deactivation of the excited state by a rotation around the C–NH_2 bond. Nevertheless, the fluorescence intensity increases significantly upon DNA addition (Fig. 2B) (51). Notably, the fluorescence enhancement is much more pronounced upon addition of (poly[dA–dT]–poly[dA–dT]) than with (poly[dC–dG]–poly[dC–dG]) or ct DNA. It was proposed that in (poly[dG-dC]-poly[dG-dC]), two effects with opposite results take place: a) the emission intensity increases due

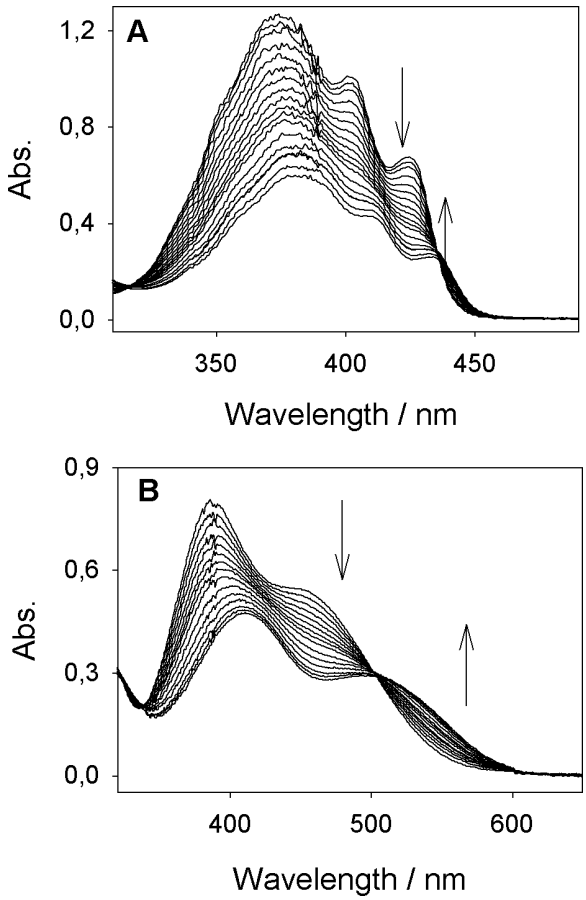

Figure 1. Spectrophotometric titration of benzoquinolizinium **9b** (**A**) and **9c** (**B**) with ct DNA in phosphate buffer (0.01 M, pH = 7.0, T = 25°C); [**9b**] = [**9c**] = 10^{-4} M; titration interval: 0.5 molar equivalents of DNA; arrows indicate the development of the absorption band upon addition of DNA. Figure 1A adapted from (51) with kind permission of Royal Society of Chemistry. Figure 1B adapted from (53).

to conformational restriction and b) the emission intensity decreases due to a PET reaction with the guanine bases. Since the latter effect is not possible in AT-rich regions, a much higher fluorescence is observed therein.

The data from the spectrophotometric and spectrofluorometric titrations were used to estimate the corresponding binding constants according to the model of McGhee and von Hippel (Table 1).

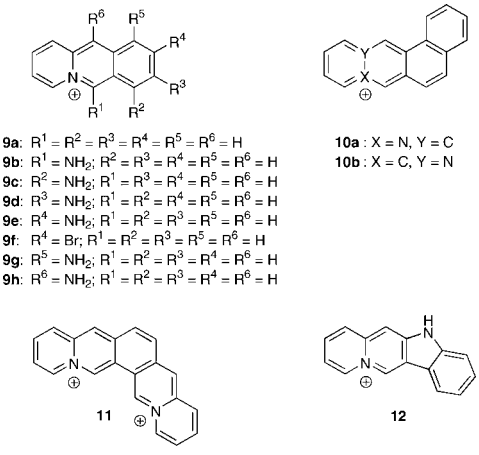

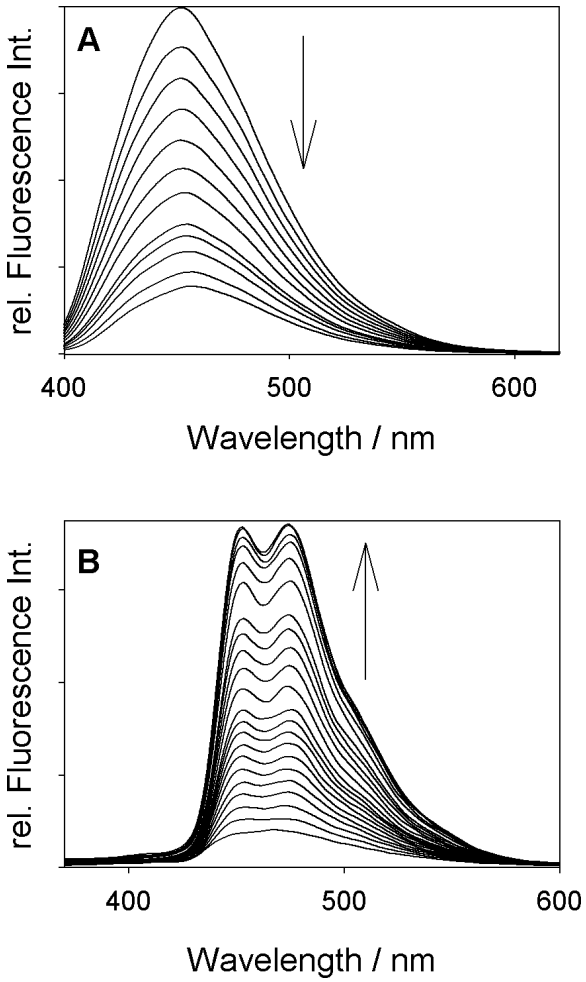

Figure 2. Spectrofluorometric titration of benzoquinolizinium **12** (**A**) and indoloquinolizinium **9b** (**B**) with ct DNA in phosphate buffer (0.01 M, pH = 7.0, T = 25°C); [**12**] = [**9b**] = 10^{-5}M; titration interval: 0.5 molar equivalents of DNA; arrows indicate the development of emission band upon DNA titration. Figure 2A adapted from (47) with kind permission of Wiley-VCH Publishers. Figure 2B adapted from (51) with kind permission of Royal Society of Chemistry.

Although the binding constants do not show a structure-property correlation, a trend may be deduced. Thus, simple benzo-annelated quinolizinium derivatives (**9**) have binding constants of *ca.* 10^4 M^{-1}, whereas the binding constants of naphtho- and indolo-annelated systems **10** and **12** and the one of the pentacyclic dication **11** are approximately one order of magnitude higher. The latter observation may be explained by an enhanced interaction between DNA base pairs and the π system, since it was shown for artificial π-stacked systems that the extension of the π surface by one benzene moiety increases the binding energy about 0.4 kcal/mol (55). In some cases (**9a**,**d**), the binding site size, n, is significantly larger than the one expected for an exclusive intercalative binding. In the latter case it is expected that n is approximately 4, as one binding pocket consists of 4 bases. This result already hints that in the case of **9a** and **9d** binding modes other than intercalation may contribute to the overall binding situation. It was shown exemplarily that the quinolizinium derivatives **9a**, **9b**, **9e**, **10a**, **10b** and **12** exhibit a slight binding selectivy for GC-rich DNA as shown by the comparison of binding constants with (poly[dC–dG]–poly[dC–dG]) and (poly[dA–dT]–poly[dA–dT]).

The interactions of quinolizinium derivatives **9–12** with DNA were further evaluated by CD spectroscopy. For example, buffered aqueous solutions of the benzo-annelated quinolizinium salts **9a**, **9e** and **12** have no CD activity, but an induced circular dichroism (ICD) was observed on addition of DNA to these salts (Fig. 3). Such ICD signals result from a nondegenerate coupling of the dye chromophore with the DNA-base transitions (56). The CD spectra of **9a**, **9e** and **12** in the presence of DNA differ in phase and intensity; but in each case the ICD bands in the UV–visible absorption bands of the chromophores in the absence of DNA. As the DNA bases do not absorb in this region, the ICD bands originate from the complexed dye. Most quinolizinium salts exhibit a positive ICD signal between 300 and 450 nm when bound to the nucleic acid; however, the amino-substituted acridizinium salt **9e** gives a weak negative ICD signal in the presence of DNA at dye-to-DNA ratios smaller than 0.05. Moreover, at a higher dye-to-DNA ratio (> 0.1) a bisignate signal pattern appears for the long-wavelength absorption band of **9e**. Presumably, under these conditions the dye forms aggregates along the DNA backbone (''outside stacking'') which leads to exciton coupling within these aggregates. In general, the resulting exciton CD signals have higher intensities than do the ICD signals of the intercalated molecules and may overlap with the latter.

The appearance of an ICD signal confirms the dye–DNA interaction and may provide further information about the position of a dye in its complex with DNA, because the intensity and the phase of the ICD signal is dependent on the position and the orientation of the chromophore relative to the DNA bases. In general, an intercalator has a weak and negative ICD signal when its transition moment is polarized along the long axis of the binding pocket (that is parallel to the bisector of the base pairs). On the other hand, relatively strong positive ICD bands appear when the transition moment is polarized perpendicular to the long axis of the binding pocket. Groove binders give even more intense ICD signals and usually exhibit a positive band. Although no experimental or theoretical data exist for the distinct orientation

Table 1. Shift of absorption maximum, Δλ, binding constants, K, and binding-site size, n, from spectrometric titration of quinolizinium derivatives with DNA in phosphate buffer (10 mM, pH = 7.0) or in ETN-buffer (10 mM; pH = 7.0)

	Native DNA[a]			(poly[dC-dG]–poly[dC-dG])		(poly[dA-dT]–poly[dA-dT])	
	Δλ[b]/ nm	K/ [$M^{-1} \times 10^4$]	n/ bases[e]	K/ [$M^{-1} \times 10^4$]	n/ bases[e]	K/ [$M^{-1} \times 10^4$]	n/ bases[e]
9a[c,f]	4	1.2	10	5.7	4.0	0.8	9.4
9b[c,g]	8	2.8	4.5	12	1.8	2.8	3.8
9c[c,h]	10	11	2.6				
9d[c,f]	20	5.2	6.2				
9e[c,f]	12	6.2	4.0	9.2	4.0	3.4	8.4
9h[c,h]	13	1.9	3.8				
10a[d,i]	11	19	5.2	56	2.8	13	6.4
10b[d,i]	12	21	5.2	54	2.6	9.0	6.4
11[d,j]	12	57	5.6	300	3	0.6	9
12[d,k]	4	15	3.4	42	3.2	12	7.8

[a] ct DNA: **9b**, **9c**, **9h**; st DNA: **9a**, **9d**, **9e**, **10a**, **10b**, **11**, **12**; [b]shift relative to absorption in the absence of DNA; [c]estimated from spectrophotometric titrations; [d]estimated from spectrofluorometric titrations; [e]binding site size given as average number of nucleic bases which are occupied by one bound molecule; [f]ref. 48; [g]ref. 51; [h]ref. 53; [i]ref. 50; [j]ref. 52, [k]ref. 49.

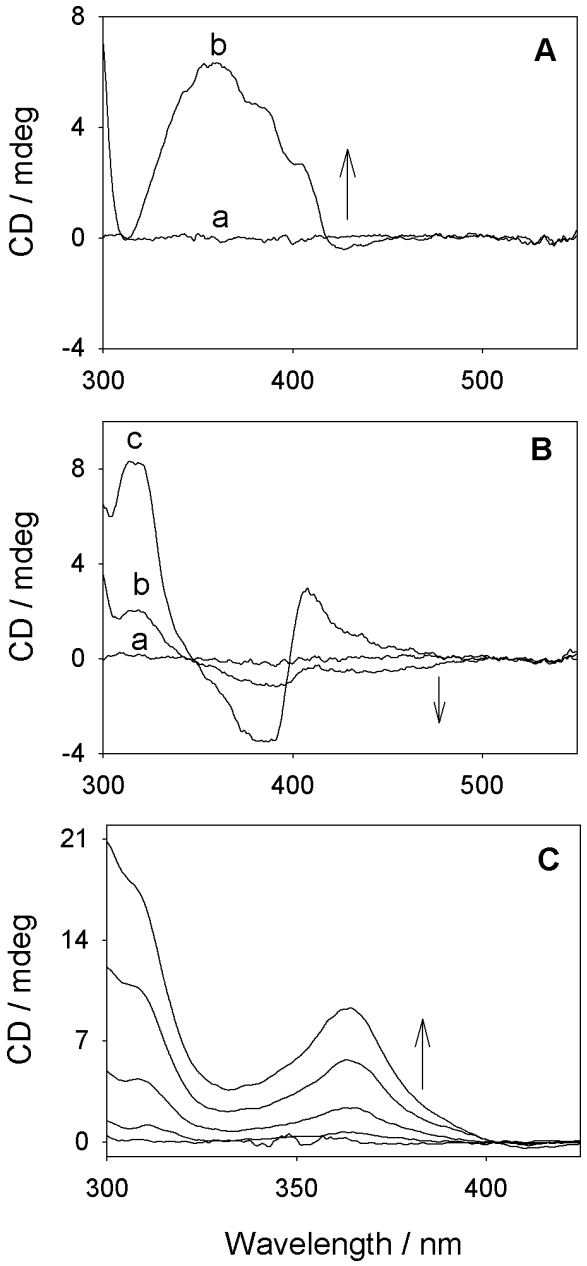

Figure 3. CD spectra of quinolizinium derivatives **9a** (**A**), **9e** (**B**), and **12** (**C**) in the presence of DNA, [DNA] = 5.7×10^{-3} M in each case; quinolizinium-to-DNA ratio, **A**: a = 0, b = 0.1; **B**: a = 0, b = 0.05, c = 0.1; **C**: arrow indicates change of ratio, 0, 0.05, 0.1, 0.15, 0.2. Figure 3A and 3B adapted from (48). Figure 3C adapted from (47) with kind permission of Wiley-VCH Publishers.

of the transition dipole moment of quinolizinium derivatives, for compounds **9e** and **12** it may be assumed that due to the donor–acceptor interplay within the chromophore the transition dipole moment of the long-wavelength absorption is aligned almost parallel to the long molecule axis. Considering this assumption the weak negative ICD band of **9e** reveals an alignment of the dye with the long-molecule axis parallel to the binding pocket, whereas **12** is oriented with the long-molecule axis perpendicular to the binding pocket. In the latter case this structure of the complex was confirmed by molecular-modeling data (49).

The binding mode of quinolizinium salts **9–12** was also evaluated by flow LD spectroscopy. Representative results are shown in Fig. 4. In general, the LD spectra of all ligand–DNA complexes exhibit negative signals for the DNA-base absorption, *i.e.* between 230–300 nm. Notably, a large increase of the LD signal intensity was obtained in the presence of most derivatives, which reflects a better orientation of the DNA in the flow field because of a pronounced stiffening of the DNA helix upon binding of the quinolizinium ion. The LD signals of all investigated quinolizinium–DNA complexes are negative in the long-wavelength absorption region of the annelated quinolizinium chromophore (300–550 nm) depending on the substitution pattern (57). Such a negative LD signal is a reliable indicator for the intercalation of the quinolizinium ions into the DNA; however, with these data additional minor-groove binding cannot be excluded. The latter is usually indicated by a weak positive LD signal which is commonly overlapped by the much stronger signals of intercalated compounds in a heterogeneous binding situation. In these cases the reduced LD (LD_r = LD/A) spectra provides additional information about the average orientation of the ligand transitions relative to the DNA bases' transitions. In general, LD_r signals of one absorption band exhibit a steady signal intensity, except in the regions of overlap between different polarizations. The latter case is observed once intercalation and groove binding take place at the same time. Along these lines the quinolizinium derivatives may be divided into a group of ''pure'' intercalators and a group of DNA binders that intercalate along with a particular degree of minor-groove association. For example, compound **9e** exhibits a constant LD_r band between 350 and 500 nm and may thus be classified as a pure intercalator. In contrast, the LD_r spectrum of **9a** shows a significant variation over the absorption-band intensity, which most likely results from a heterogeneous binding distribution.

ANNELATED AZAQUINOLIZINIUM DERIVATIVES

The replacement of a methylene group next to the quaternary nitrogen atom of quinolizinium derivatives with another nitrogen atom gives azaquinolizinium derivatives, which were also shown to bind to DNA (58–61). Thus, in detailed studies, the indolo-annelated azaquinolizinium cations **13a–f** were shown to intercalate into DNA with binding constants of $K \approx 10^5$ M^{-1}. Similarly to quinolizinium derivatives the binding event is indicated by a significant redshift of the absorption maximum ($\Delta\lambda$ = 10–16 nm) upon DNA addition with a binding site size of $n \approx 4$ (in bases). The comparison of several alkylated derivatives did not lead to a distinct correlation between substitution pattern and DNA-binding properties. Additional evidence for an intercalative binding mode was provided by viscosimetric studies, which reveal a significant increase of the DNA contour length, and unwinding studies with plasmid DNA, which show a significant propensity of **13a** and **13f** to unwind supercoiled circular DNA. Most notably, significant associative interactions of derivatives with an extended π system such as **14** and **15** could not be detected. In a following study naphtho- and benzo-naphtho-annelated azaquinolizinium salts **16** and **17** were studied with an emphasis on their topoisomerase I-inhibiting and antiproliferative activity (61). The interaction of these compounds with DNA was evaluated by titration to plasmid DNA and monitoring of the resulting dynamic topological changes by gel electrophoresis. Along with spectrophotometric titrations these experiments reveal a strong intercala-

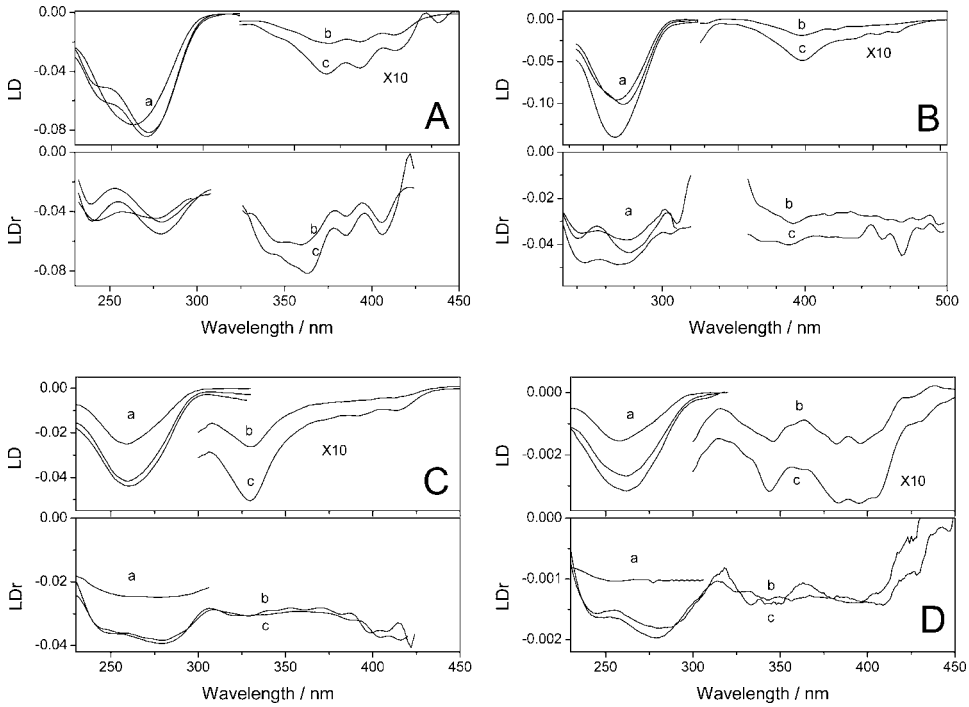

Figure 4. LD(A), and LD_r (B) spectra of mixtures of st DNA and quinolizinium derivatives **9a** (A), **9e** (B), **10a** (C), and **11** (D); **9e**, **10a**, **11**: [quinolizinium]/[DNA] = 0 (a), 0.04 (b), and 0.08 (c); **9a**: [quinolizinium]/[DNA] = 0.02 (a), 0.04 (b); all experiments in ETN buffer, 10 mM, pH = 7.0. Figure 4A and 4B adapted from (48). Figure 4C adapted from (50) with kind permission of Royal Society of Chemistry. Figure 4D adapted from (52) with kind permission of ARKAT USA Inc.

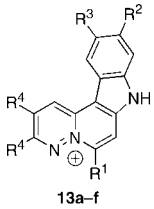

13a: $R^1 = R^2 = R^3 = H$; $R^4 = Me$
13b: $R^1 = R^4 = Me$; $R^2 = R^3 = H$
13c: $R^1 = R^2 = R^3 = R^4 = Me$
13d: $R^1 = R^2 = R^3 = H$; $R^4 = Me$
13e: $R^1 = Me$; $R^2 = R^3 = H$; $R^4 = Et$
13f : $R^1 = R^2 = R^3 = Me$; $R^4 = Et$

13a–f

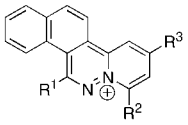

16a: R^1 = Ph; $R^2 = R^3 = H$
16b: R^1 = Ph; R^2 = Me; R^3 = H
16c: R^1 = Ph; R^2 = H; R^3 = Me
16d: R^1 = 4′-EtO-Ph; R^2 = Me; R^3 = H

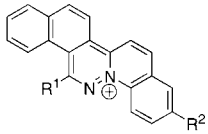

17a: R^1 = Ph; R^2 = H
17b: R^1 = Ph; R^2 = Me
17c: R^1 = 4′-EtO_2C-Ph; R^2 = H
17d: R^1 = 4′-EtO_2C-Ph; R^2 = Me

tion of **16a** and **17a–d,** whereas the other derivatives exhibit only a weak, negligible interaction with DNA. It was shown that azaquinolizinium derivatives **17a**, **17b** and **17d** inhibit topoisomerase I activity. The authors state that the mechanism of topoisomerase inhibition does not involve trapping of the cleavage complex, *i.e.* in contrast to coralyne derivatives (*vide supra*), **17a**, **17b** and **17d** do not act as topoisomerase poisons. In addition, it was shown that all derivatives exhibit to a varying extent an antiproliferative activity against selected tumor cell lines. A remarkable result of these studies is the observation that azaquinolizinium derivatives such as **16c**, which do not intercalate into DNA, have the same activity as intercalating derivatives, *e.g.* **16a**. Thus, the intuitive proposal that strong intercalators should have the highest biological activity seems to be too simplified.

In another recent study, the interaction of acenaphtho- and phenanthreno-annelated azaquinoliziniumderivatives **18** and **19** with DNA was investigated by spectrometric titrations, viscosimetry and equilibrium dialysis studies (60). In representative experiments, the association with DNA was detected by a hypsochromic effect and a redshift of the UV band ($\Delta\lambda \approx 10$ nm) upon addition of the nucleic acid. Nevertheless, isosbestic points were not observed, which indicates the formation of at least two different dye–DNA complex structures, presumably with different binding modes. The fluorescence of the azaquinolizinium derivatives **18** and **19** is quenched in the presence of DNA; however, a shift of emission wavelength was not observed. As in the case of benzo- and naphtho-annelated quinolizinium derivatives, the quenching is most likely due to an electron transfer reaction between the nucleic

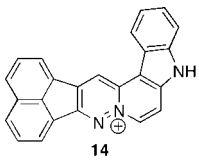

14

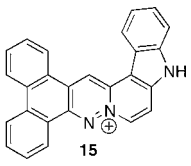

15

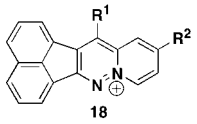

18

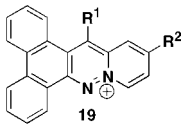

19

18a; **19a**: $R^1 = R^2 = H$
18b; **19b**: R^1 = Ph; R^2 = H
18c; **19c**: R^1 = H; R^2 = Me

bases and the excited quinolizinium. Additional viscosimetric titrations reveal that the viscosity of aqueous DNA solutions increases upon addition of **18** or **19**, which indicates an intercalative binding mode.

SUMMARY AND OUTLOOK

Considering the increasing contribution of cancer to the overall mortality rate, the design and application of novel drugs with efficient and selective antitumor activity is an urgent task in medicinal chemistry. It may be argued that any monodirectional approach in cancer therapy is unlikely to provide efficient treatment, *i.e.* synergistic effects between several different approaches may be required. Nevertheless, the DNA-binding properties of a drug may play a key role in its application in antitumor chemotherapy, so the understanding of DNA association and the design of DNA-binding drugs are significant contributions to cancer therapy. We hope that we were able to show that in this context annelated quinolizinium ions represent a useful and versatile platform for the design of DNA intercalators and are a promising lead structure of DNA-targeting drugs. Studies of the biological properties of coralyne and its derivatives have already shown that these compounds exhibit a high potential to interfere efficiently with tumor-cell proliferation and presumably further research along these lines may lead to the successful application of such compounds in chemotherapy. Nevertheless, for this purpose major drawbacks need to be solved first. Thus the tendency of coralyne and its derivatives to form aggregates needs to be suppressed, because such aggregation may hinder the delivery of the drug to the target. In addition, a method for the penetration of these rather hydrophilic compounds through the lipophilic cell membrane needs to be provided, because even the best intercalating drug does not exhibit increased cell toxicity without appropriate absorption into the cell. These two examples already demonstrate the need for structural variation of quinolizinium derivatives in order to obtain desired functionality. Nevertheless, it should be emphasized that annelated quinolizinium derivatives are readily available and their substitution patterns may be easily varied by routine operations of organic chemistry. Thus, it should be worthwhile to explore further the potential of these intercalating molecules and integrate them into new concepts and designs for tumor-targeting drugs, *e.g.* as functional part in *bis*-intercalators in compounds that bind to abasic sites.

Acknowledgements—This work was generously financed by the Deutsche Forschungsgemeinschaft, the Deutscher Akademischer Austauschdienst (Vigoni-Programme), the Universitätsbund Würzburg and the Fonds der Chemischen Industrie. H.I. thanks all his coworkers from the ''quinolizinium group,'' namely Milena Bressanini, Verena Deutloff, Dr. Katja Faulhaber, Anton Granzhan, Andrea Hofmann, Hubert Kraußer, Daniela Otto, Astrid Salbach and Andreas Schmitt (''Schmitti''), for their fruitful discussions and their skillful, dedicated work, and Prof. Waldemar Adam and Dr. Chantu Saha-Möller, University of Würzburg, for the encouragement to focus on this research topic.

REFERENCES

1. Lerman, L. S. (1961) Structural considerations in the interaction of deoxyribonucleic acid and acridines. *J. Mol. Biol.* **3**, 18–30.
2. Lerman, L. S. (1963) The structure of the deoxyribonucleic acid (DNA)-acridines complex. *Proc. Natl. Acad. Sci. U.S.A* **49**, 94–102.
3. Hurley, L. H. (2002) DNA and its associated processes as targets for cancer therapy. *Nat. Rev. Cancer* **2**, 188–200.
4. Graves, D. E. and L. M. Velea (2000) Intercalative binding of small molecules to nucleic acids. *Curr. Org. Chem.* **4**, 915–929.
5. Brana, F. M., M. Cacho, A. Gradillas, B. Pascual-Teresa and A. Ramos (2001) Intercalators as anticancer drugs. *Curr. Pharm. Des.* **7**, 1745–1780.
6. Haq I. and J. Ladbury (2000) Drug-DNA recognition: energetics and implications for design. *J. Mol. Recognit.* **13**, 188–197.
7. Thurston, D. E. (1999) Nucleic acid targeting: therapeutic strategies for the 21st century. *Br. J. Cancer* **80**, 65–85.
8. Dervan P. B., A. T. Poulin-Kerstien, E. J. Fechter and B. S. Edelson (2005) Regulation of gene expression by synthetic DNA-binding ligands. *Top. Curr. Chem.* **253**, 1–32.
9. Wilson W. D. (1996) Reversible interactions of nucleic acids with small molecules. In *Nucleic Acids in Chemistry and Biology* (Edited by G. M. Blackburn and M. J. Gait), pp. 329–374. IRL Press, Oxford, UK.
10. Geierstanger, B. H. and D. E. Wemmer (1995) Complexes of the minor-groove of DNA. *Annu. Rev. Biophys. Biomol. Struct.* **24**, 463–493.
11. Demeunynck, M., C. Bailly and W. D. Wilson (2002) *DNA and RNA Binders*. Wiley-VCH, Weinheim.
12. Armstrong R. W., T. Kurucsev and U. P. Strauss (1970) Interaction between acridine dyes and deoxyribonucleic acid. *J. Am. Chem. Soc.* **92**, 3174–3181.
13. Tuite E. and B. Nordén (1994) Sequence specific interactions of methylene blue with polynucleotides and DNA: A spectroscopic study. *J. Am. Chem. Soc.* **116**, 7548–7556.
14. LePecq J.-B. and C. Paoletti (1967) A fluorescent complex between ethidium bromide and nucleic acids–physical-chemical characterization. *J. Mol. Biol.* **27**, 87–106.
15. Netzel T. L., K. Nafisi, M. Zhao, J. R. Lenhard and I. Johnson (1995) Base-content dependence of emission enhancements, quantum yield, and lifetimes for cyanine dyes bound to double-strand DNA: Photophysical properties of monomeric and bichromophoric DNA stains. *J. Phys. Chem.* **99**, 17936–17947.
16. Rye H. S., S. Yue, D. E. Wemmer, M. A. Quaesada, R. P. Haugland, R. A. Mathies and A. N. Glazer (1992) Base-content dependence of emission enhancements, quantum yields, and lifetimes for cyanine dyes bound to double-strand DNA: photophysical properties of monomeric and bichromomphoric DNA stains. *Nucleic Acids Res.* **20**, 2803–2812.
17. Hannah, K. C. and B. A. Armitage (2004) DNA-templated assembly of helical cyanine dye aggregates: a supramolecular chain polymerization. *Acc. Chem. Res.* **37**, 845–853.
18. Cantor, C. R. and P. R. Schimmel (1980) *Biophysical Chemistry, Part II*, pp. 392–463. W. H. Freeman and Co., San Francisco.
19. Nordén B., M. Kubista and T. Kurucsev (1992) Linear dichroism spectroscopy of nucleic acid. *Q. Rev. Biophys.* **25**, 51–171.
20. Suh, D. and J. B. Chaires (1995) Criteria for the mode of binding of DNA binding agents. *Biorg. Med. Chem.* **3**, 723–728.
21. Medhi, C., J. B. O. Mitchell, S. L. Price and A. B. Tabor (1999) Electrostatic factors in DNA intercalation. *Biopolymers* **52**, 84–93.
22. Ihmels, H. (2004) Quinolizinium salts and benzo analogues. In *Science of Synthesis, Volume 15: Six-Membered Hetarenes with One Nitrogen or Phosphorus Atom,* (Edited by D. Black), pp. 907–946. Georg Thieme Verlag, Stuttgart.
23. Philips, S. D. and R. N. Castle (1988) A review of the chemistry of the antitumor benzo[*c*]phenantridine alkaloids nitidine and fagaronine and of the related antitumor alkaloid coralyne. *J. Heterocyclic Chem.* **18**, 223–232.
24. Gupta, R. S., W. Murray and R. Gupta (1988) Cross resistance pattern toward anticancer drugs of a human carcinoma multidrug-resistant cell-line. *Br. J. Cancer* **58**, 441–447.
25. Gatto, M., M. M. Sanders, C. Yu, H. Y. Yu, D. Makhey, E. J. LaVoie and L. F. Liu (1996) Identification of topoisomerase I as the cytotoxic target of the protoberberine alkaloid coralyne. *Cancer Res.* **56**, 2795–2800.
26. Zee-Cheng, K. Y. and C. C. Cheng (1973) Interaction between DNA and coralyne acetosulfate, an antileukemic compound. *J. Pharm. Sci.* **62**, 1572–1573.
27. Wilson, W. D., A. N. Gough, J. J. Doyle and M. W. Davidson (1976) Coralyne. intercalation with DNA as a possible mechanism of antileucemic action. *J. Med. Chem.* **19**, 1261–1263.
28. Gough, A. N., R. L. Jones and W. D. Wilson (1979) Dimerization of coralyne and its propyl analog and their association with DNA. *J. Med. Chem.* **22**, 1551–1554.
29. Pal, S., G. S. Kumar, D. Debnath and M. Maiti (1998) Interaction of the antitumor alkaloid coralyne with dublex deoxyribonucleic acid structures: spectroscopic and viscosimetric studies. *Ind. J. Biochem. Biophys.* **35**, 321–332.
30. Keppler, M., S. Neidle and K. R. Fox (2001) Stabilization of TG- and AG-containing antiparallel DNA triplexes by triplex-binding ligands. *Nucleic Acids Res.* **29**, 1935–1942.

31. Lee, J. S., L. J. P. Latimer and K. J. Hampel (1993) Coralyne binds tightly to both T•A•T- and C•G•C+-containing DNA triplexes. *Biochemistry* **32**, 5591–5597.
32. Moraru-Allen, A. A., S. Cassidy, J.-L. Asensio Avarez, K. R. Fox, T. Brown and A. N. Lane (1997) Coralyne has a preference for intercalation between TA•T triples in intramolecular DNA triple helices. *Nucleic Acids Res.* **25**, 1890–1896.
33. Polak, M. and N. V. Hud (2002) Complete disproportionation of duplex poly(dT)•poly(dA) into triplex poly(dT)•poly(dA)•poly(dT) and poly(dA) by coralyne. *Nucleic Acids Res.* **30**, 983–992.
34. Jain, S. S., M. Polak and N. V. Hud (2003) Controlling nucleic acid secondary structure by intercalation: effects of DNA strand length on coralyne-driven duplex disproportionation. *Nucleic Acids Res.* **31**, 4608–4615.
35. Persil, Ö., C. T. Santai, S. S. Jain and N. V. Hud (2004) Assembly of an antiparallel homo-adenine DNA duplex by small-molecule binding. *J Am. Chem. Soc.* **126**, 8644–8645.
36. Albergo, D. D. and D. H. Turner (1981) Solvent effects on the thermodynamics of double-helix formation in $(dG\text{-}dC)_3$. *Biochemistry* **20**, 1413–1418.
37. Chen A. Y. and L. F. Liu (1994) DNA topoisomerases—essential enzymes and lethal targets. *Annu. Rev. Pharmacol.* **34**, 191–218.
38. Wang J. C. (1996) DNA topoisomerases. *Annu. Rev. Biochem.* **65**, 635–692.
39. Wang, L.-K., B. D. Rogers and S. M. Hecht (1996) Inhibition of topoisomerase I function by coralyne and 5,6-dihydrocoralyne. *Chem. Res. Toxicol.* **9**, 75–83.
40. Hsiang, Y.-H. and L. F. Liu (1988) Identification of mammalian DNA topoisomerase I as an intracellular target of the anticancer drug camptothecin. *Cancer Res.* **48**, 1722–1726.
41. Pilch, D. S., C. Yu, D. Makhey, E. J. LaVoie, A. R. Srinivasan, W. K. Olson, R. S. Sauers, K. J. Breslauer, N. E. Geacintov and L. F. Liu (1997) Minor groove-directed and intercalative ligand-DNA interactions in the poisoning of human DNA topoisomerase I by protoberberine analogs. *Biochemistry* **36**, 12542–12553.
42. Yu, Y., C.-Y. Long, S.-Q. Sun and J.-P. Liu (2001) Application of an alkaloid as a novel fluorescence probe in the determination of DNA. *Anal. Lett.* **34**, 2659–2669.
43. Makhey, D., B. Gatto, C. Yu, A. Liu, L. F. Liu and E. J. LaVoie (1996) Coralyne and related compounds as mammalian topoisomerase I and topoisomerase II poisons. *Bioorg. Med. Chem.* **4**, 781–791.
44. Caprasse, M. and C. Houssier (1984) Physico-chemical investigation of the mode of binding of the alkaloids 5,6-dihydroflavopereirine and sempervirine. *Biochimie* **66**, 31–41.
45. Martin, M. A., B. Del Castillo and D. A. Lerner (1988) Study of the luminescence properties of a new series of quinolizinium salts and their interaction with DNA. *Anal. Chim. Acta* **205**, 105–115.
46. Ihmels, H., K. Faulhaber, B. Engels and C. Lennartz (2000) New dyes based on amino-substituted acridizinium salts—synthesis and exceptional photochemical properties. *Chem. Eur. J.* **6**, 2854–2864.
47. Ihmels, H., K. Faulhaber, K. Wissel, G. Bringmann, K. Messer, G. Viola and D. Vedaldi (2001) Synthesis and investigation of the DNA-binding and DNA-photodamaging properties of indolo-[2,3-b]-quinolizinium bromide. *Eur. J. Org. Chem.*, **2005** 1157–1161.
48. Ihmels, H., K. Faulhaber, C. Sturm, G. Bringmann, K. Messer, N. Gabellini, D. Vedaldi and G. Viola (2001) Acridizinium salts as a novel class of DNA-binding and site-selective DNA-photodamaging chromophores. *Photochem. Photobiol.* **74**, 505–511.
49. Viola, G, F. Dall'Acqua, N. Gabellini, S. Moro, D. Vedaldi and H. Ihmels (2002) Indolo[2,3-b]-quinolizinium bromide: an efficient intercalator with DNA-photodamaging properties. *Chem. BioChem.* **3**, 550–558.
50. Viola, G., M. Bressanini, N. Gabellini, D. Vedaldi, F. Dall'Acqua and H. Ihmels (2002) Naphthoquinolizinium derivatives as novel platform for DNA-binding and DNA-photodamaging chromophores. *Photochem. Photobiol. Sci.* **1**, 882–889.
51. Ihmels, H., K. Faulhaber, K. Wissel, G. Viola and D. Vedaldi (2003) 6-Aminoacridizinium bromide: a fluorescence probe which lights up in AT-rich regions of DNA. *Org. Biomol. Chem.* **1**, 2999–3001.
52. Viola, G., H. Ihmels, H. Kraußer, D. Vedaldi and F. Dall'Acqua (2004) DNA-binding and DNA-photocleavaging properties of 12a,14a-diazoniapentaphene. *ARKIVOC* **5**, 219–230.
53. Faulhaber K. (2003) Untersuchunger der Wechselwirkungen von anellierten Chinoliziniumsalzen mit DNA. Dissertation, University of Würzburg, Germany. Available at: http://opus.bibliothek.uni-wuerzburg.de/opus/volltexte/2003/679/. Accessed on 23 May 2005.
54. Bohne, C., K. Faulhaber, B. Giese, A. Häfner, A. Hofmann, H. Ihmels, A.-K. Köhler, S. Perä, F. Schneider and M. A. L. Sheepwash (2005) Studies on the mechanism of the photoinduced DNA damage in the presence of acridizinium salts—involvement of singlet oxygen and an unusual source for hydroxyl radicals. *J. Am. Chem. Soc.* **126**, 76–85.
55. Rebek J. (1990) Molecular recognition with model system. *Angew. Chem., Int. Ed. Engl.* **29**, 245–255.
56. Nordén, B. and T. Kurucsev (1994) Analysing DNA complexes by circular and linear dichroism. *J. Mol. Recognit.* **7**, 141–156
57. Saraf, S.-U.-D. (1981) Absorption spectra of benzologs of quinolizinium ions. *Heterocycles* **16**, 987–1007.
58. Molina, A., J. J. Vaquero, J. L. Garcia Navio, J. Alvarez-Builla, M. M. Rodrigo, O. Castano and J. L. J. Andres (1996) Azonia derivatives of the γ-carboline system, a new class of DNA intercalators. *Bioorg. Med. Chem. Lett.* **13**, 1453–1456.
59. Molina, A., J. J. Vaquero, J. L. Garcia Navio, J. Alvarez-Builla, B. Pascual-Teresa, F. Gago, F. and M. M. Rodrigo (1999) Novel DNA intercalators based on the pyrazino[1′,6′:1,2]pyrido[4,3-b]indol-5-inium system. *J. Org. Chem.* **64**, 3907–3915.
60. Martin, M. A., A. S. Bouin, S. Muñez-Botella and B. del Castillo (2002) A study of the interaction of polycyclic derivatives of azaquinolizinium salts with DNA. *Polycyclic Aromatic Compounds* **22**, 37–53.
61. Martinez, V., C. Burgos, J. Alvarez-Builla, G. Fernandez, A. Domingo, R. Garcia-Nieto, F. Gago, I. Manzanares, C. Cuevas and J. J. Vaquero, (2004) Benzo[*f*]azino[2,1-*a*]phthalazinium cations: novel DNA intercalating chromophores with antiproliferative activity *J. Med. Chem.* **47**, 1136–1148.